PHYSICAL REVIEW A VOLUME 7, NUMBER 1 JANUARY 1973

Investigations in Many-Body Perturbation Theory of Hyperfine Structure in Diatomic Molecules*

James E. Rodgers, Taesul Lee, and T. P. Das
Department of Physics, State University of New York, Albany, New York 12222
and
Dennis Ikenberry
Department of Physics, California State College, San Bernardino, California 92407
(Received 2 June 1972)

The linked-cluster many-body perturbation theory has been applied to small heteronuclear diatomic molecules using a variational Hartree–Fock molecular-orbital basis set. This procedure has been applied to study the isotropic hyperfine interaction in the $^2\Pi$ ground state of the free radical $O^{17}H$ and to the magnetic shielding of H^1 and F^{19} in the HF molecule. These investigations have led to a number of physical conclusions about the influence of correlation and exchange polarization effects on the isotropic hyperfine interactions in OH. The calculated shielding parameters and hyperfine constants were found to be in better than 15% agreement with experimental data wherever available.

I. INTRODUCTION

The linked-cluster many-body perturbation theory (LCMBPT) has been applied successfully to study the various bound-state properties of atoms such as their energies, hyperfine constants, polarizabilities, and related properties.[1] In principle, the theory is readily extendible to molecular systems, but in practice the multicenter nature of the latter makes it difficult to obtain the basis states needed for perturbation calculations. To circumvent this difficulty about basis-set wave functions for LCMBPT calculations, some recent approaches have utilized[2] zero-order one-center Hamiltonians as the starting point for which one can obtain the complete set of states by numerical solution as in atoms. This procedure has provided[2] fairly accurate total and correlation energies in a number of molecules. However, the accuracy of this procedure for properties such as hyperfine interactions which depend on the immediate vicinity of the nuclei has yet to be tested, particularly at peripheral nuclei which are not at the center of expansion. Since one starts in this case with a zero-order wave function whose amplitudes at the nuclei are expected to be significantly different from the actual molecular wave function, one expects higher-order perturbation effects to be substantial. Additionally, for homonuclear molecules, the one-center Hamiltonian is expected to be rather different from the real Hamiltonian and could lead to convergence problems even for the energy.

It appears, therefore, that to attain versatility in handling both varieties of properties and varieties of molecules by the LCMBPT procedure, one has to explore the possibilities of using multicenter basis sets. One, of course, has to use variational methods to determine these basis functions since the multicenter equations for the wave functions cannot be solved conveniently by numerical integration. Recently, Schulman and Kaufman[3] have utilized linear combinations of Gaussian atomic orbitals to generate the basis set for LCMBPT calculations of the indirect spin-spin interaction constant in the HD molecule. However, with the Gaussian representation, one requires a significantly larger number of functions to represent the the molecular wave functions than is the case for Slater orbitals. The latter have been used[4] extensively to obtain self-consistent-field (SCF) (Hartree–Fock–Roothaan) wave functions for the occupied states of molecules. For the two molecules OH and HF that we have chosen for our present investigations, the basis sets involving the occupied states and unoccupied excited states were available[5] from Hartree–Fock–Roothaan calculations for the occupied states. The unoccupied molecular orbitals arise as a consequence of the large variational atomic-orbital basis sets which were used in these calculations. Since the aim of the calculations[5] from which these basis sets were obtained was to determine good Hartree–Fock–Roothaan wave functions for the occupied states, the one-electron Hamiltonian used was a Hartree–Fock Hamiltonian involving what is known in many-body literature[6] as a V^N potential. Consequently, the unoccupied or excited states of the one-electron Hamiltonian, which are referred[6] to as particle states, all have energies greater than zero and lie in the continuum. In the literature on many-body perturbation theory in atoms, the V^{N-1} potential has been the more popular choice as the zero-order potential and is found to lead to better convergence for polarizabilities . In one atomic system, namely, $He^3(^3S)$, LCMBPT calculations with a V^N basis have led to reasonable agreement with ex-

periment for the contact hyperfine constant.[7] Recently, other choices of zero-order potentials have been tested[8] for the perturbation procedure. Since accurate basis sets of states are currently available for the V^N potential in molecules, one is in a position to study the nature of the results one obtains with their use in many-body perturbation calculations. In addition to the intrinsic interest of these results, one can obtain from them some insight into the physical and computational aspects of the perturbation approach which should be valuable for investigations with other potentials.

Our choice of OH and HF molecules has been dictated by the following considerations. We wanted to study two classes of molecular systems, one involving unpaired electrons that would have finite hyperfine interaction in the first order as in finite-spin atomic systems and a second class which would be diamagnetic, but have data available on chemical shifts associated with one order in magnetic hyperfine interaction and one order in the magnetic field. The OH free radical is a good candidate for the first class, in addition to being of astrophysical interest.[9] The HF molecule is a good candidate for the second class.[10] Both of these molecular systems are small enough that one can carry out a detailed analysis of the theory of their hyperfine properties without an inordinate amount of effort. In addition, there was the fortunate circumstance mentioned above that their excited states were available from Cade and Huo's calculations.[5]

II. RÉSUMÉ OF FORMALISM AND METHOD OF CALCULATION

The LCMBPT method as applied to atoms has been described in a number of places.[1] The formulation for applying it to molecules is broadly the same and therefore only a few basic points will be included here with a few remarks that are characteristic of molecules.

What we are seeking is the exact solution of the Schrödinger equation for the molecule, namely,

$$H\Psi = E\Psi$$

in the Born–Oppenheimer approximation. In trying to obtain this objective by the perturbation procedure, we split the Hamiltonian H into a zero-order part H_0 and a perturbation part H', namely,

$$H = H_0 + H' .$$

In the present work, H_0 is the Roothaan–Hartree–Fock Hamiltonian.[11] This is the counterpart of the Hartree–Fock V^N Hamiltonian for atomic systems, with specific choices[11] for certain parameters for Fock operators for open-shell systems.

In LCMBPT, the exact wave function Ψ is given by the linked-cluster expansion

$$\Psi = \sum_n^L \left(\frac{H'}{E_0 - H_0}\right)^n \Phi_0 , \tag{1}$$

where Φ_0, the "vacuum" state in this formalism, is the eigensolution of the zero-order equation

$$H_0\Phi_0 = E_0\Phi_0 , \tag{2}$$

and the symbol L indicates that only linked terms in the perturbation series are to be retained. For the hyperfine constant, which is a one-electron property, one needs the expectation value of a one-electron operator, in this case the hyperfine Hamiltonian operator $H'_{\rm hfs}$, over the wave function Ψ, leading to

$$\langle H'_{\rm hfs}\rangle = \sum_{n,m}^L \langle \Phi_0 | [H'(E_0 - H_0)^{-1}]^n \times H'_{\rm hfs}[(E_0 - H_0)^{-1}H']^m | \Phi_0\rangle . \tag{3}$$

Following the usual field-theoretic–type prescription,[1] a typical term in the summation in Eq. (3) can be written in terms of a set of linked diagrams of order (n, m). For the case of nuclear magnetic shielding[12] in the HF molecule, one needs to include in addition to the orbital hyperfine operator, the operator describing the perturbation due to an external magnetic field. A convenient way of doing this is to include the magnetic field perturbation H'_H in H' and keep all terms in Eq. (3) which involve one order of H'_H.

As indicated earlier in the Introduction, the one-electron basis set of states that we have used was obtained[5] in the process of performing Hartree–Fock–Roothaan calculations for the ground states of these molecules. The many-electron zero-order wave function Φ_0 is obtained by the occupation of the lowest-energy one-electron states, in keeping with the symmetry of the ground state, as in the case of atoms. The unoccupied one-electron states were then handled as excited or "particle" states. The number of excited levels available is 20 for both molecules OH and HF, composed of 13 of σ symmetry and 7 of π symmetry. Since the number of basis functions is finite and since they were obtained variationally rather than by exact numerical solution, one might be concerned about their completeness. To test this property, we utilized the procedure of checking the equality of the left- and right-hand sides of the matrix-product equation:

$$\langle A | O | A\rangle = \sum_n \langle A | O | n\rangle\langle n | A\rangle ,$$

where O is a one-electron operator and $|A\rangle$ is a one-electron function, the summation over n running over the entire basis set. Using for $|A\rangle$ several choices of Slater functions based on the oxygen or fluorine atoms and the hydrogen atom and $O = 1$, $1/r$, $\delta(\vec{r})$, z, and r (with the origin of r

taken both with respect to H and the other atom), the completeness test[13] was found to be well satisfied.

The evaluation of the many-body diagrams requires the calculation of a number of one- and two-electron matrix elements over the basis states, the operator involved in the latter case being $1/r_{12}$. The two-center integrals involved in these calculations were obtained using the α-function technique first developed by Löwdin[14] and extended[15] subsequently by Ikenberry, Sharma, and Duff. This allows convenient programing of α-function expansions of wave functions of any l about the initial center and to any number of desired l components about the second center. In view of the substantial size of the atomic basis sets involved in the linear-combination-of-atomic-orbital (LCAO) expansion of the molecular basis orbitals used here, the evaluation of the two-electron matrix elements over the molecular basis sets required careful programing with special storage techniques to economize on the computer time and make most efficient use of available memory on the UNIVAC 1108.

III. RESULTS AND DISCUSSION

As pointed out in the Introduction, our present work falls broadly into two categories, the isotropic hyperfine-interaction constant in the free radical OH and the nuclear magnetic shielding constants for H^1 and F^{19} nuclei. In this section, our results will be presented in this order. In the former case, for economy of space, only diagrams with contributions greater than a certain minimum will be presented and the net contribution through second order in electron-electron interactions will be included. In the latter case, electron-electron interactions will only be included through first order. In both cases, our results will be compared with available experiment and earlier theoretical results obtained through other procedures.

A. Isotropic Hyperfine Interaction in OH

As discussed in Sec. II, for the expectation value of one-electron operators including many-body effects, the pertinent expression is Eq. (3). For the hyperfine-interaction problem at hand, the pertinent one-electron operator is the Fermi-contact hyperfine Hamiltonian for nucleus N:

$$H'_{\rm hfs} = \frac{8\pi}{3}\,\frac{g_N\mu_N}{a_B^3}\,g_e\mu_B\,\vec{I}_N\cdot\sum_i \vec{s}_i\,\delta(\vec{r}_{iN})\ . \tag{4}$$

Noting that the experimental hyperfine spin-Hamiltonian is usually written as

$$H_{\rm spin} = 2\pi\hbar A(N)\,\vec{I}_N\cdot\vec{S}\ ,$$

the expression for the hyperfine constant $A(N)$ in Hz for nucleus N is given in terms[16] of linked-diagram contributions by

$$A(N) = \frac{1}{2\pi\hbar I_N S}\sum_{n,m}^{L}\langle\Phi_0(S,\,M_S=S)\,|\,[H'(E_0-H_0)^{-1}]^n \times H'_{\rm hfs}[(E_0-H_0)^{-1}H']^m\,|\,\Phi_0(S,M_S=S)\rangle\ . \tag{5}$$

In Eq. (5), $\Phi_0(S, M_S=S)$ is the vacuum-state many-electron wave function, which, in the present case, is the Hartree–Fock wave function corresponding to total spin S and $M_s=S$. The hyperfine constant will be calculated in frequency units, but for comparison of purely electronic effects for the O^{17} and H^1 nuclei, it is the spin density $\gamma(N)$, namely,

$$\gamma(N) = \sum_{n,m}^{L}\langle\Phi_0(S,M_s=S)\,|\,[H'(E_0-H_0)^{-1}]^n \times 2\sum_{s_z i}\delta(\vec{r}_{iN})\,[(E_0-H_0)^{-1}H']^m\,|\,\Phi_0(S,M_s=S)\rangle\ , \tag{6}$$

which is the more relevant quantity. In terms of $\gamma(N)$, $A(N)$ is given by

$$A(N) = F(N)\,\frac{g_e\mu_B}{2\pi\hbar}\,\gamma(N)\ , \tag{7}$$

where

$$F(N) = \tfrac{4}{3}\pi\,(g_N\mu_N/a_B^3 S)\ . \tag{8}$$

For ready reference, we list here the values of $F(N)$ for O^{17} and H^1 using the most recent physical constants[17]

$$F(O^{17}) = -216.220\ \text{Oe},\qquad F(H^1) = 1594.98\ \text{Oe}\ . \tag{9}$$

On multiplying the calculated spin density in Eq. (6) by the factors in (9) we get the hyperfine constants in units of Oe as they are often expressed in ESR work. However, if one is interested in frequency units (Hz), this can be accomplished by multiplying the result in Oe by the factor

$$g_e\mu_B/2\pi\hbar = 2.80247\ \text{MHz/Oe}\ . \tag{10}$$

For both H^1 and O^{17} nuclei in the ground $^2\Pi$ state of OH radical $(1\sigma^2 2\sigma^2 3\sigma^2 1\pi_1^2 1\pi_{-1}^*)$ there is no direct contact hyperfine interaction since the internuclear axis is a nodal line for the unpaired $1\pi_{-1}^*$ electron. As in related situations in atoms such as nitrogen and phosphorus, the hyperfine interaction arises from core-polarization and correlation effects associated with the unpaired electron.

The hyperfine diagrams for the proton are presented in Fig. 1. For economy of space, only a limited number of diagrams are presented, namely, those with contributions to the spin density greater than $0.25\times10^{-3}a_B^{-3}$. In these diagrams a wiggly line followed by the symbol C denotes the matrix element of the spin-density operator between the indicated states. In these diagrams, σ hole states are denoted by $n\sigma$ and $n'\sigma$ $(n, n'=1, 2, 3)$ and particle states by $k\sigma$ $(4\le k\le 16)$. Similarly, $1\pi_1^*$, $1\pi_1^-$, $1\pi_{-1}^*$ are hole states and $k\pi$ denotes particle states

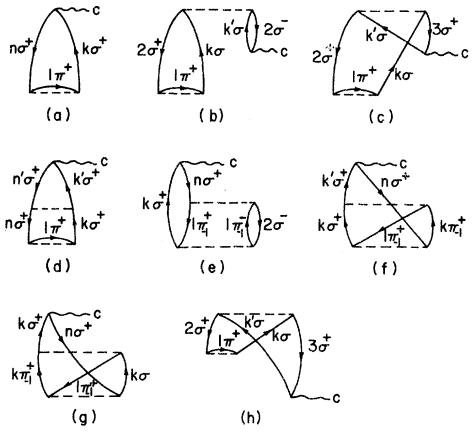

FIG. 1. Major diagrams contributing to the proton hyperfine interaction in OH.

$(2 \leq k \leq 8)$. In our work here, we have studied the diagrams involving the orders (01), (11), and (02), adding up to a total of 152 in all. Table I lists the contributions from the ones not shown.

The physical effects represented by the diagrams in Fig. 1 are broadly analogous to the corresponding atomic hyperfine diagrams.[1,18] Thus, for example, Fig. 1(a) represents the usual first-order exchange core-polarization effects of the paired σ orbitals by the unpaired $1\pi^+_{-1}$ electron. The 2σ and 3σ contributions to this diagram are of the same order of magnitude and same sign (negative), while the 1σ contribution is negligible. This smallness of the 1σ contribution is understandable since this orbital has very small density at the proton. The corresponding situation at O^{17} is, however, markedly different as will be discussed later.

TABLE I. Contributions to the hyperfine interaction at the proton in OH. Values are given in terms of the electronic spin density at H^1, in a.u. $\times 10^{-3}$ (see Fig. 1).

	Diagram	Spin-density contribution
1(a)	$n\sigma = 2\sigma$	−7.33
	$n\sigma = 3\sigma$	−2.48
1(b)		−0.39
1(c)		−1.21
1(d)	$n\sigma = n'\sigma = 2\sigma$	−2.03
	$n\sigma = n'\sigma = 3\sigma$	−0.86
1(e)	$n\sigma = 2\sigma$	0.52
	$n\sigma = 3\sigma$	−0.27
1(f)	$n\sigma = 2\sigma$	0.25
	$n\sigma = 3\sigma$	0.48
1(g)	$n\sigma = 3\sigma$	−0.34
1(h)		0.38
Total of all (0,1)		−9.81
Total of all (1,1)		−1.37
Total of all (0,2)		−2.80
Net spin density		−13.98

Figures 1(b) and 1(c) are of order (1, 1) and represent the combined influence of core polarization and intrashell and intershell interactions among the paired orbitals, respectively. Diagrams 1(d)–1(g) are of order (0, 2) with 1(d) being related to the core-polarization diagram 1(a) by the introduction of an additional order of a σ-σ radial correlation. Figure 1(e) is analogous to the "phase-space" diagrams of atomic hyperfine literature and is the result of the asymmetry in the correlation effects from σ states of opposite spin due to the presence of an empty $1\pi^-_{-1}$ state. Diagrams 1(f) and 1(g) represent the influence of the correlation between σ states and the unpaired π state. Finally, Fig. 1(h) is similar in form to the (11) diagram 1(c) but, due to different time ordering, is referred to as a (02) diagram.

From Table I, the total spin density at the proton through second order in electron-electron interactions is seen to be -14.0×10^{-3} a.u. which is composed of −0.0098, −0.0014, and −0.0028 from (01), (11), and (02) orders. Using the requisite conversion factor, the total spin density corresponds to a hyperfine constant $A(H) = -65.52$ MHz. For ready reference, the (01), (11), and (02) contributions to the hfs constants have also been listed in MHz in Table III.

The hyperfine diagrams for O^{17} are presented in Fig. 2 with corresponding contributions in Table II. Again, for economy of space, only diagrams representing spin densities greater than about $5\times10^{-3}a_B^{-3}$, or 5% of the total calculated quantity, are shown in Fig. 2. Figure 2(a) again represents the core-polarization contribution. In contrast to

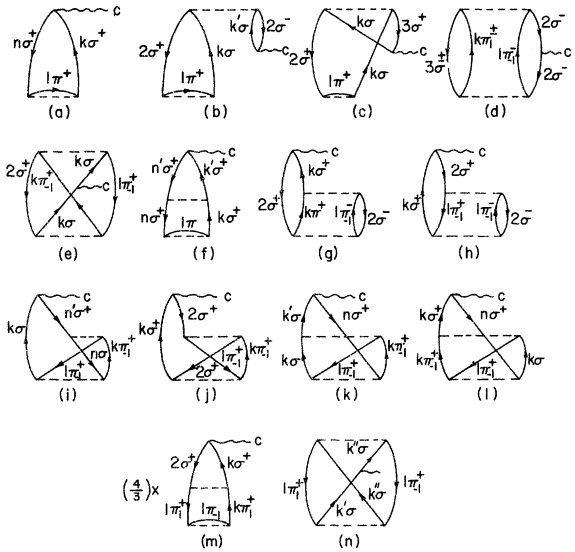

FIG. 2. Major diagrams contributing to the O^{17} hyperfine interaction in OH.

TABLE II. Contributions to the hyperfine interaction at oxygen nucleus in OH. The spin density is in a.u. $\times 10^{-3}$ (see Fig. 2).

	Diagram	Spin-density contribution
2(a)	$n\sigma = 1\sigma$	−167.48
	$n\sigma = 2\sigma$	180.35
	$n\sigma = 3\sigma$	15.77
2(b)		11.47
2(c)		−6.53
2(d)	+exchange	8.47
2(e)		−5.97
2(f)	$n\sigma = n\sigma' = 1\sigma$	−19.76
	$n\sigma = n\sigma' = 2\sigma$	51.40
	$n\sigma = n\sigma' = 3\sigma$	5.22
	$n\sigma = 2\sigma$, $n'\sigma = 1\sigma$	7.31
	$n\sigma = 2\sigma$, $n'\sigma = 3\sigma$ +vice versa	5.28
2(g)		7.48
2(h)		−11.73
2(i)	$n\sigma = n'\sigma = 1\sigma$	−7.35
	$n\sigma = 2\sigma$, $n'\sigma = 3\sigma$	12.49
2(j)		6.65
2(k)	$n\sigma = 2\sigma$	−11.14
2(l)		−5.86
2(m)		14.47
2(n)		−4.32
Total of all (0,1)		28.63
Total of all (1,1)		19.02
Total of all (0,2)		54.12
Net spin density		101.77

the situation for the H^1 hyperfine constant, the 1σ contribution is now large and negative and cancels the major part of the positive contribution from the 2σ state which is augmented by a relatively small but positive contribution from the 3σ state. The large negative contribution from the 1σ state can be explained by the movement of the closely packed parallel spin electron away from the nucleus as a result of the exchange attraction of the unpaired π electron. This leaves a surplus negative spin density at the nucleus. For the 2σ and 3σ states, the electronic distribution is more diffuse and peaked not far from the maxima of the unpaired 1π density and, in contrast to the 1σ case, it is difficult to predict qualitatively which direction the parallel spin density will be moved by exchange. The order-of-magnitude-larger spin density observed for the 2σ state relative to 3σ is probably a consequence of the combination of relatively greater density at the nucleus in the former case as well as a stronger exchange with the unpaired electron.

Of the second order (11) and (02) [Figs. 2(a)–2(n)] diagrams 2(b), 2(c), 2(f), 2(h), 2(k), and 2(l) represent the same physical effects as diagrams 1(b)–1(g) for the proton hfs. Considering these latter five diagrams first, there are some differences in the natures of the contributions in the case of O^{17} as compared to the proton. Thus, in diagram 2(f), the contribution from $n\sigma = n'\sigma = 1\sigma$ is appreciable now in contrast to the case of the proton where it was negligible due to the small density of the 1σ orbital at the proton site. Additionally, in the case of O^{17}, the off-diagonal components of diagram 2(f), corresponding to $n \neq n'$, are of greater relative importance compared to the diagonal diagrams, in contrast to the situation at the proton. Also diagrams 2(k) and 2(l) are now of greater relative importance when referred to diagram 2(a) than the counterparts in the case of the proton.

Considering the rest of the diagrams in Fig. 2, 2(d), 2(e), 2(g), 2(i), 2(j), 2(m), and 2(n) do have their counterparts for the proton (Fig. 1) but were not exhibited there because they made relatively small contributions. Of these diagrams for O^{17}, diagram 2(d) and its exchange version with particle lines crossed represent the effect of asymmetric correlation between the 2σ and 3σ orbitals for states with different spin. (The empty $1\pi_{-1}^{-}$ state is available as an excited state for only the down-spin state.) Figure 2(e) represents the influence of correlation between the σ states and the unpaired $1\pi_{-1}^{+}$ state. Diagram 2(m) is analogous to diagram 2(f) but involves π-π exchange instead of π-σ. It is to be noted that the multiplying factor $\frac{4}{3}$ for this diagram is characteristic of the Roothaan approximation[11] to the starting Hartree–Fock potential for open-shell molecules and would be different for a different choice. Diagrams 2(g), 2(i), and 2(j) are broadly similar to diagrams 2(h), 2(k), and 2(l), respectively, in that the second interaction line is connected between hole states in one case and between particle states in the other.

In general, the diagrams for O^{17} resemble more closely the diagrams for the second-period atoms[18–20] than is the case for the H^1 diagrams. This is not surprising since the electronic environment of O^{17} in OH is similar to that for an oxygen atom. In particular, the close cancellation between 1σ and the combined 2σ and 3σ contributions is analogous to the cancellation between $1s$ and $2s$ core-polarization contributions to the hfs of boron, nitrogen, and oxygen atoms.

The total spin density at oxygen is seen from Table II to be $101.8 \times 10^{-3} a_B^{-3}$ of which 28.6, 19.0, and 54.1 ($\times 10^{-3} a_B^{-3}$) arise from (0,1)-, (11)-, and (02)-type diagrams, respectively. Using the appropriate conversion factor from Eq. (9), we get the hyperfine constant for O^{17} as $A(O) = -61.67$ MHz, composed of the (01), (11), and (02) contributions listed in Table III.

Unfortunately, no experimental value is available for the O^{17} hfs constant. The experimental value[21] of the H^1 hfs constant is $A(H) = -74.6 \pm 0.6$ MHz. Our theoretical result is in reasonable agreement

TABLE III. Calculated hyperfine constants by order in perturbation theory. Values given are in MHz and apply to the specific isotopes H^1 and O^{17}.

Order	O^{17} (MHz)	H^1 (MHz)
(0,1)	−17.35	−43.85
(1,1)	−11.52	−6.13
(0,2)	−32.79	−12.54
Total, $A(N)$	−61.67	−62.52

with this value. We shall remark on the source of the difference later in this section, after discussing the other available theoretical calculations.[22,23] Both of these are configuration interaction calculations, one using two-center basis sets[22] and the other one-center[23] sets. The first of these calculations,[22] involving two-center molecular orbitals and aimed only at the proton hfs, utilized, for configuration interaction, excited configurations obtained from one available empty σ state in addition to the occupied states. Since no configurations involving excited π states were included, this calculation cannot include the influence of diagrams of the type 1(f) and 1(g) for H^1 and 2(d), 2(g), 2(i), 2(j), and 2(m) for O^{17}. In addition, diagrams of the type 1(e) for the proton were also excluded. Since this calculation was concerned mainly with the H^1 hfs constant, the omission of π excitations may be seen from Table I to be not as serious as it would have been for O^{17} (see Table II). However, since only a single excited σ state was used and we have found comparable contributions from a number of additional excited states, it is difficult to assess the theoretical accuracy of the calculated result −67.9 MHz. Two-center configuration-interaction (CI) studies using more than one excited state would be very desirable in this respect.

In the one-center CI calculation[23] which has been done, excited σ orbitals were used. Since no excited π orbitals were employed, again the contribution of π-excitation diagrams is absent. The theoretical results obtained in this calculation were −11.2 MHz for H^1 and two alternate values −1.4 and −99.3 MHz for O^{17}. As the author has remarked, not much weight is to be attached to the H^1 result because the orbitals were expanded about the oxygen center. The first O^{17} result is obtained using all ten excited σ orbitals to build excited configurations, while for the second O^{17} result, two of these orbitals were dropped from a consideration of the reasonableness of their densities at the O^{17} nucleus. The second result agrees more favorably with our result. However, an examination of the spin-density contributions from single-excitation core-polarization effects indicates that there is better accord with our results when the full set was used. In particular, the 1σ contribution, in this case, is opposite in sign and comparable in magnitude to the 2σ and 3σ contributions as we found for diagram 2(a).

B. Magnetic Shielding of H^1 and F^{19} Nuclei in HF Molecule

In the molecule OH studied in Sec. III A, there was an unpaired electron present which produced a contact hyperfine interaction, albeit through its correlation and exchange polarization effects on the paired orbitals. On the other hand, the HF molecule involves spin-paired states and does not have a finite hyperfine constant. The hyperfine effect that we are interested in for this molecule is the magnetic shielding coefficient which arises from the interplay of the orbital perturbation by a magnetic field and the orbital hyperfine interaction. In the perturbation formalism that we are employing, as symbolized by Eq. (3), the influence of the magnetic field perturbation (H_H') is incorporated by including H_H' in H' and computing the expectation value of the orbital hyperfine operator.

Variational methods that have been applied[12(b),24,25] to the shielding problem fall into two categories. In one of these categories,[12(b)] the effect of electron-electron interaction is ignored and one studies the perturbations of the one-electron orbitals individually due to the magnetic field. This corresponds to what is denoted as method C in Langhoff, Karplus, and Hurst's (LKH) (Ref. 26). In the second category,[12(b),25] corresponding to the method A in the language of LKH, one includes the influence of electron-electron interactions as a self-consistency effect in the perturbed state. In our present calculation, we have included the diagrams which specifically include these consistency effects. To describe the diagrams, one has first to consider the perturbation Hamiltonian relevant to the present problem. The perturbation terms involving the magnetic field and nuclear-moment perturbations can be obtained by considering[27] the interaction between the electron and the magnetic vector potential due to both the nuclear moment and the applied magnetic field. The form of these perturbation terms depends on the choice of origin (gauge) used for the vector potential for the magnetic field, but from gauge-invariance arguments the net answer for the shielding constant is expected to be independent of this choice.

In the present work, since the major part of the electron density is on the fluorine atom, we have chosen the fluorine nucleus as the origin for the magnetic field perturbation. For the perturbation due to the nuclear moment, the origin is chosen at either the proton or the fluorine nucleus, depending upon the one whose shielding is being studied. With this choice, the zero-order Hamiltonian H_0 and perturbation Hamiltonian, composed of four terms H_1 through H_4, are given by

$$H_0 = \frac{1}{2m}\sum_i p_i^2 + V_0 ,$$

$$H_1 = \sum_{i>j}\frac{1}{r_{ij}} - V^N ,$$

$$H_2 = -\frac{e\hbar}{2mc}\vec{H}\cdot\left(\sum_i (\vec{r}_i - \vec{R})\times\vec{p}_i\right), \qquad (11)$$

$$H_3 = -\frac{e\hbar}{mc}\vec{\mu}\cdot\sum\frac{\vec{l}_i}{r_i^3} ,$$

$$H_4 = \frac{e^2}{2m^2c^2}\vec{\mu}\cdot\sum\left(\frac{\vec{r}_i\vec{r}_i - r_i^2\overleftrightarrow{1} + \vec{r}_i\cdot\vec{R}\,\overleftrightarrow{1} - \vec{r}_i\vec{R}}{r_i^3}\right)\cdot\vec{H} ,$$

where V_0 is the one-electron potential involving the electron-nuclear Coulomb interaction and the Hartree–Fock V^N interaction between the electrons. The position vector for the electron, namely, $\vec{r}_i$, is measured from the nucleus under study, and $\vec{R}$ is the radius vector joining the same nucleus to the origin of the magnetic vector potential. Note that $\vec{R}=0$ for the fluorine nucleus and is the internuclear vector $\vec{H}\vec{F}$ for the proton. The vectors $\vec{l}_i$ and $\vec{p}_i$ are the angular and the linear momenta, with $\vec{l}_i$ measured with respect to the particular nucleus under study. In addition to these perturbation terms, there are two others involving μ^2 and $\vec{H}^2$, respectively, which are not of interest in the present problem.

The magnetic shielding tensor $\overleftrightarrow{\sigma}$ for the nucleus of magnetic moment $\vec{\mu}$ in the uniform magnetic field $\vec{H}$ is then defined by the usual relation[28]

$$\Delta E(\mu, H) = -\vec{\mu}\cdot(\overleftrightarrow{1} - \overleftrightarrow{\sigma})\cdot\vec{H} , \qquad (12)$$

where $\Delta E(\mu, H)$ represents the sum of energy terms that involve both $\vec{\mu}$ and $\vec{H}$ simultaneously to one order each. Conventionally, the part σ^d of σ given by

$$\overleftrightarrow{\sigma}^d = \frac{e^2}{2mc^2}\langle 0|\sum_i\frac{r_i^2\overleftrightarrow{1} - \vec{r}_i\vec{r}_i}{r_i^3}|0\rangle \qquad (13)$$

is termed[27] the diamagnetic shielding term, the balance $\overleftrightarrow{\sigma}$ being defined as the paramagnetic term. With the choice of gauge as in Eq. (11), $\overleftrightarrow{\sigma}^p$ is given by

$$\overleftrightarrow{\sigma}^p = -\frac{e^2}{2mc^2}\langle 0|\sum_i\frac{\vec{r}_i\cdot\vec{R}\,\overleftrightarrow{1} - \vec{r}_i\vec{R}}{r_i^3}|0\rangle + (\text{perturbation terms involving one order each in } H_2 \text{ and } H_3). \qquad (14)$$

The wave function $|0\rangle$ refers to the many-particle wave function involving in principle all orders in H_1, as given by Eq. (1). Similarly, the other perturbation terms in Eq. (14) also involve all orders in H_1 and are obtained using Eq. (3) with $H' = H_1 + H_2$ and $H'_{\rm hfs} = H_3$.

Experimentally, the absolute shielding tensor $\overleftrightarrow{\sigma}$ is not available, since one usually measures only the chemical shift with respect to a standard reference system. On the other hand, one can get a measure of $\overleftrightarrow{\sigma}^p$ experimentally by relating it to the rotational magnetic field.[29] Since HF is a linear molecule, $\sigma_{xx} = \sigma_{yy}$ and $\sigma_{zz} = 0$, z being the direction of the internuclear axis. In the literature, it is conventional to quote the motionally averaged paramagnetic shielding constant $\sigma^p = \frac{2}{3}\sigma^p_{xx}$, which is what we shall use here for both experimental and theoretical numbers.

The diagrams for σ^p involving up to one order in the electron-electron interaction are presented in Fig. 3. These diagrams are evaluated for the magnetic field in the x direction. The pertinent one-electron operators associated with H_2, H_3, and H_4 are thus l_{xF}, l_{xA}/r_A^3, and $-R_{zA}/r_z^3$ (A = F or H). The vertices associated with these operators are shown in Fig. 4. Since the diagrams are all evaluated in atomic units, we need the same conversion factor $\alpha^{2/3}$ for all the diagrams where α is the fine-structure constant.

Figure 3(a) represents the first term of σ^p, in Eq. (14), a summation being taken over all the occupied σ and π states. This diagram only contributes to the proton shielding. Figure 3(b) represents the perturbation contributions from the individual states through one order each in H_2 and H_3. It represents the effects that one obtains through method C of LKH used in some of the earlier variation calculations.[24]

Figures 3(c)–3(e), combined with the various possible time orderings of the H_2 and H_3 operators, represent the consistency effects that occur in method A of LKH[26] in carrying out second-order polarizability-type calculations. These effects have been incorporated in some of the more recent variational calculations.[12(b),25] The contributions from these five diagrams for the proton and fluorine nuclei are tabulated in Table IV. Figure 3(a) has a vanishing contribution for the F^{19} nucleus. For the proton, it is the major contributor. Figures 3(b) and 3(c) make an order-of-magnitude-larger contribution for fluorine than for the proton. This is understandable, since the magnetic field perturbation is centered at fluorine where most of the charge density is located and hence the perturbation of this charge density provides a much stronger field at the fluorine nucleus than at the proton which is more distant from the region where the perturbation occurs. The same explanation holds for the even larger difference in relative effects from the

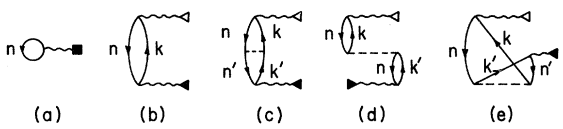

FIG. 3. Diagrams contributing to the paramagnetic shielding constants in HF.

higher orders for the two nuclei . The net paramagnetic shielding constants obtained from these five diagrams for the fluorine and the proton are listed in the last line of Table IV.

The experimental values for σ^p from rotational magnetic field data[30] are $(-6.79 \pm 0.4) \times 10^{-5}$ and -7.96×10^{-5} for fluorine and the proton, respectively. Thus, the agreement between our theoretical value for fluorine and the experimental value is within 15%. For the proton, the theoretical result is in closer agreement (within 4%) with the experimental result. The nature of this agreement is quite reasonable considering that only one order in the electron-electron interaction was included in the diagrams in Fig. 3. Comparison can be made with two recent variational calculations of the shielding constants that included consistency effects. In one of these calculations, a variational function was used[25] which involved essentially a single parameter related to excitation to a 4σ state. The values obtained in this latter calculation are -7.570×10^{-5} and -7.058×10^{-5}, respectively, for fluorine and proton. For purposes of comparison, we have evaluated our contribution to σ^p for fluorine from all the diagrams in Fig. 3 using only the single 4σ excited state and find the result to be -7.21×10^{-5}. This result compares reasonably well with that of Ref. 25 considering the fact that the two calculations used different wave functions for the occupied and excited (4σ) states. The other[12(b)] self-consistent variational calculation for σ^p used a number of additional wave functions besides the occupied ones to expand the perturbed wave function needed to obtain the second-order energy involving μH. Their values for σ^p in fluorine and the proton[31] were -6.771×10^{-5} and -7.92×10^{-5}, respectively, in very good agreement with experiment. We feel that this better agreement obtained in Ref. 12(b) with experiment, as compared to our results, is a consequence of their using a substantial-sized basis set comparable in dimension to the one we have used and the fact that consistency effects can be incorporated to higher orders through the variational procedure.

IV. CONCLUDING REMARKS

The LCMBPT procedure with molecular-orbital V^N basis sets has been applied in this paper to study hyperfine properties for two diatomic molecules OH and HF and found to give agreement to better than 15% with available experimental data.

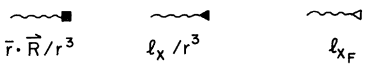

FIG. 4. Vertices for the magnetic shielding diagrams in Fig. 3.

TABLE IV. Contributions to σ^p from the diagrams in Fig. 3 in units of $\sigma^p \times 10^5$.

Diagram		F	H
3(a)	$n=1\sigma$		
	$n=2\sigma$		
	$n=3\sigma$		
	$n=1\pi$		
	Subtotal	0	−7.2972
3(b)	$n=1\sigma$	0	0
	$n=2\sigma$	0.0256	−0.1866
	$n=3\sigma$	1.3603	−0.5122
	$n=1\pi$	−6.1227	0.2761
	Subtotal	−4.7368	−0.4227
3(c)	$n=n'=1\sigma$	0	0
	$n=n'=2\sigma$	0.0078	−0.0150
	$n=n'=3\sigma$	0.4516	−0.0749
	$n=n'=1\pi$	−3.6594	0.1834
	$n\neq n'$	0.1083	−0.0355
	Subtotal	−3.0012	0.0580
3(d)		0.1332	−0.0042
3(e)		−0.2900	−0.0007
Total		−7.8948	−7.668

These investigations have led to certain physical conclusions about the origin at hyperfine properties (which provide a sensitive test of the wave function) which should be helpful for future improved calculations on the present systems and other molecules. For example, one of the observations that we have made from our diagrams as discussed in Sec. III is that the isotropic hyperfine constant on the proton in OH is quite significantly influenced by correlation effects. The same is true of the O^{17} hyperfine constant but this is, of course, expected. Another interesting effect observed was the close cancellation for O^{17} of the exchange core-polarization effects associated with the 1σ orbitals and the combined effect of the 2σ and 3σ orbitals. This effect is analogous to the corresponding cancellation between $1s$ and $2s$ states in open-shell atoms of the second period.

The remaining discrepancies between experiment and theory for the H^1 hyperfine constant in OH and between the H^1 and F^{19} paramagnetic shielding constants and experiment most likely arise from higher-order effects in the electron-electron interaction. A preliminary examination of higher-order diagrams indicates that their contributions do not converge as well as in the case of atoms, and we feel that this is a consequence of the use of the V^N potential which does not have any bound excited states. However, reasonable success has been achieved in this work up to second order with basis states available from Roothaan–Hartree–Fock calculations on molecular ground states. This

provides encouragement for investing the time and effort needed for calculation of hyperfine properties through the use of V^{N-1} or other basis sets which include bound excited states.

---

*Work supported by the National Science Foundation.

[1]See, for example, T. Lee, N. C. Dutta, and T. P. Das, Phys. Rev. A 1, 995 (1970); 4, 1410 (1971), and references therein; H. P. Kelly and A. Ron, *ibid.* 2, 1261 (1970); see O. Sinanoglu and K. A. Brueckner, *Three Approaches to Electron Correlation in Atoms* (Yale U. P., New Haven, Conn., 1970) for a discussion of the various many-body approaches to electronic structure in atoms and molecules.

[2]H. P. Kelly, Phys. Rev. Letters 23, 455 (1969); T. Lee, N. C. Dutta, and T. P. Das, *ibid.* 25, 204 (1970); H. P. Kelly and J. H. Miller, *ibid.* 26, 679 (1971); Phys. Rev. A 4, 480 (1971); T. Lee and T. P. Das, Bull. Am. Phys. Soc. 17, 69 (1971); for complete calculations, see Phys. Rev. A 6, 968 (1972).

[3]J. Schulman and D. N. Kaufman, J. Chem. Phys. 53, 477 (1970).

[4]See, for example, A. C. Wahl, J. Chem. Phys. 41, 2600 (1964); Phys. Rev. A 4, 825 (1971); P. E. Cade, R. F. W. Bader, and J. Pelletier, J. Chem. Phys. 54, 3517 (1971); J. Schamps and H. Lefebvre-Brion, *ibid.* 56, 573 (1972).

[5]P. E. Cade and W. M. Huo, J. Chem. Phys. 47, 614 (1967). We are very grateful to Professor Cade for providing these basis sets for us.

[6]H. P. Kelly, Phys. Rev. 136, B896 (1964).

[7]N. C. Dutta, C. Matsubara, R. T. Pu, and T. P. Das, Bull. Am. Phys. Soc. 13, 674 (1968).

[8]J. M. Schulman and W. S. Lee, Phys. Rev. A 5, 13 (1972); J. M. Schulman, W. S. Lee, S. S. Hui, and J. I. Musher, *ibid.* (to be published); S. Huzinaga and C. Arnau, *ibid.* 1, 1285 (1970); J. H. Miller and H. P. Kelly, *ibid.* 3, 578 (1971).

[9]See, G. Herzberg, *The Spectra and Structure of Simple Free Radicals* (Cornell U. P., Ithaca, N. Y., 1971), and references therein; also B. E. Turner, Astron. Astrophys. 2, 453 (1969); A. Churg and D. H. Levy, Astrophys. J. 162, L161 (1970).

[10]N. F. Ramsey, *Molecular Beams* (Oxford U. P., New York, 1956); see also, S. I. Chan and T. P. Das, J. Chem. Phys. 37, 1527 (1962).

[11]C. C. J. Roothaan, Rev. Mod. Phys. 32, 179 (1960).

[12]See, for example, (a) T. P. Das and R. Bersohn, Phys. Rev. 115, 897 (1959); (b) R. M. Stevens and W. N. Lipscomb, J. Chem. Phys. 41, 184 (1964); (c) J. I. Musher, Rev. Mod. Phys. 39, 203 (1967).

[13]A similar test was carried out by Schulman and Kaufman for an H_2 molecule. See Ref. 3.

[14]P. O. Löwdin, Advan. Phys. 5, 1 (1956).

[15]D. Ikenberry (unpublished); R. R. Sharma, J. Math. Phys. 9, 505 (1968); K. J. Duff, Intern. J. Quantum Chem. 5, 111 (1971).

[16]T. Lee, N. C. Dutta, and T. P. Das, Phys. Rev. A 1, 995 (1970).

[17]B. N. Taylor, W. H. Parker, and D. N. Langenberg, Rev. Mod. Phys. 41, 375 (1969).

[18]In fact, the diagrams for OH are essentially the same as those which occur for the atomic boron $^2P_{3/2}$ state except for some modifications due to the extra occupied paired state in OH. Complete report is unpublished and is in the Ph.D. dissertation of one of the authors (J.E.R.) (University of California, Riverside, August, 1972).

[19]H. P. Kelly, Phys. Rev. 173, 142 (1968); 180, 55 (1969).

[20]N. C. Dutta, C. Matsubara, R. T. Pu, and T. P. Das, Phys. Rev. 177, 33 (1969).

[21]H. E. Radford, Phys. Rev. 122, 114 (1961); 126, 1035 (1962).

[22]K. Kayama, J. Chem. Phys. 39, 1507 (1963).

[23]A. L. Chung, J. Chem. Phys. 46, 3144 (1967).

[24]See Ref. 12(a); H. J. Kolker and M. Karplus, J. Chem. Phys. 41, 1259 (1964)

[25]D. Zeroka and H. F. Hameka, J. Chem. Phys. 45, 300 (1966).

[26]P. W. Langhoff, M. Karplus, and R. P. Hurst, J. Chem. Phys. 44, 505 (1966).

[27]A. Abragam, Nuovo Cimento Suppl. 6, 1015 (1957) [see also Ref. 12(a)].

[28]N. F. Ramsey, *Molecular Beams* (Clarendon, Oxford, England, 1956).

[29]N. F. Ramsey, Phys. Rev. 78, 699 (1950); 83, 540 (1951); 86, 243 (1952).

[30]S. I. Chan and T. P. Das, J. Chem. Phys. 37, 1527 (1962); J. N. Pinkerton and C. H. Anderson, Bull. Am. Phys. Soc. 6, 281 (1961); M. R. Baker, H. M. Nelson, J. A. Leavitt, and N. F. Ramsey, Phys. Rev. 121, 807 (1961).

[31]The value of σ^p at the proton was obtained from Ref. 12(b) by using the value of the spin-rotational constant $C = 70.65$ kHz, and the usual relation (see Ref. 29):

$$\sigma^p = \tfrac{1}{3}\alpha^2\left(-\frac{z}{R} + \frac{a_B \pi (\mu' R^2) C}{M \mu_N \gamma_N}\right).$$